Numerical modelling of low-frequency acoustically induced vibration in gas pipeline systems

O. M. Silva [1], D. M. Tuozzo [1], J. G. Vargas [1], L. V. Kulakauskas [1], A. F. Fernandes [1], J. L. Souza [1], A. P. Rocha [1], A. Lenzi [1], R. Timbó [2], C. O. Mendonça [2], A. T. Brandão [2]
[1] Federal University of Santa Catarina, Multidisciplinary Optimization Group, MOPT/LVA, Campus Trindade, Florianópolis, Brazil
e-mail: **olavo@lva.ufsc.br**

[2] PETROBRAS
Ilha do Fundão, Rio de Janeiro, Brazil

Abstract
The structural vibration behavior of gas pipeline systems can be strongly affected by the response of the acoustic domain represented by the gas being transported through pressurized pipes, cylinders and other related components. The Acoustically Induced Vibration (AIV) can be a cause of failure, for example, in reciprocating compression systems. The authors present a strategy based on the acoustic Transfer Matrix Method (TMM) and on the Timoshenko beam theory to represent the acoustic-structure interaction in gas pipelines as a weakly coupled system, modeled by the Finite Element Method (FEM). It is possible to predict the dynamic behavior of pipe systems subjected to harmonic acoustic loads, with excitation frequencies similar to the first harmonics within typical compressors pulsation's spectra. An open source code called *OpenPulse* was developed in Python, where displacement, stress and pressure fields are shown in 3D graphs and associated with frequency plots. Coherent results were achieved using the proposed procedure.

1 Introduction

Petroleum, in its natural form, can not be used in a practical way for other purposes than supplying energy by combustion processes. However, its chemical composition is based on hydrocarbons of large molecular heterogeneity, enabling the production of very specialized products (petroleum derivatives) that are required in modern engines and complex industrial systems [1]. For this reason, refining processes are performed to transform and refine crude oil into useful products like Liquefied Petroleum Gas (LPG), kerosene, asphalt base, jet fuel, gasoline, heating oil, fuel oils, paraffin, petroleum coke, and many others sub-products. The refining processes can be classified as [1]:

- Separation processes (processes without chemical reactions, in which different properties are used in the separation of mixtures of different compositions): distillation, crystallization, adsorption, membrane processes, absorption, stripping, and extraction;
- Conversion processes (processes with promotion of chemical reactions to obtain hydrocarbons of economic interest): thermal and catalytic processes;
- Treating processes (processes that stabilize and upgrade petroleum sub-products by separating them from less desirable sub-products and by removing objectionable elements): amine gas and caustic treating, and hydrotreating.

Hydrotreating is a process by which pressurized hydrogen, in presence of a catalyst, reacts with sulfur compounds in the produced fuel to form hydrogen sulfide gas (H_2S) and a hydrocarbon [2]. This is one of the most important processes to improve the quality of petroleum derivatives. The resultant H_2S gas is not classified as a fine derivative, and it is eliminated through a recuperation process (the resultant "pure" sulfur, in

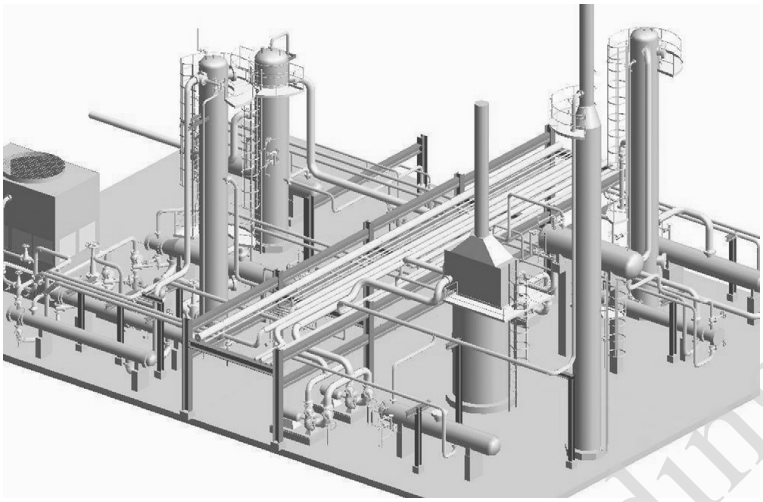

Figure 1: CAD representation of a complex piping system (source: [3]).

solid form, is exploited for other purposes like in food and cosmetic industry).

In the hydrotreating process, the hydrogen gas must be pressurized to high pressures, being transported through pipes, cylinders, and other related components. Large reciprocating compressors are used to reach this objective. The gas (acoustic fluid) pulsation produced by this kind of machine is an important source of excitation for the pipeline systems that transport the pressurized gas throughout the refinery plant.

As a consequence, the structural vibration behavior of pipeline systems can be strongly affected by the response of the acoustic domain represented by the gas being transported through the pipes. When vibrations are induced by compressor gas pulsation, the phenomenon is known as Acoustically Induced Vibration (AIV). This vibration mechanism is considered an important problem in industry because is a common cause of failure that obstructs smooth plant operations and in serious cases can lead to significant maintenance and repair costs. An example of a piping system can be seen in Fig. 1.

AIV is a vibration mechanism that responds to an unsteady fluid flow and/or to a pulsating flow field [4]. Dealing with AIV means that the general random frequency characteristic of the fluid flow in the pipes has a particular frequency component (and harmonics if broadband excitation exists) that becomes dominant when the interaction between the acoustic fluid and the compressor occurs (intermittent suction/discharge flow generating pressure pulsations or acoustic oscillations).

Reciprocating compressors or positive displacement pumps can cause these pressure pulsations, which contain many harmonic components of the rotational speed (with more energy generally in frequencies less than 100 Hz). Also, centrifugal compressors can generate tonal pressure pulsations at low flow conditions and sub-synchronous tonal pressure component (10 to 80% of rotor speed) caused by the rotating stall. The pressure pulsation can be too weak to cause any problem by itself, but if a coincidence with any acoustic and structural piping natural frequency occurs, the pulsation can be largely amplified [5], and hence significant "shaking" forces can appear.

Approximate models can be used to calculate frequency-domain solutions for AIV. The most common methods used to obtain that solutions are: the Method of Characteristics (MOC), especially used for water hammer calculations in the time-domain [6]; the Finite Element Method (FEM) [7], a powerful and well-known technique for solving problems in engineering; the Matrix Condensation Method (MCC) [8, 9]; the Transfer Matrix Method (TMM) [8, 10, 11, 5, 12], an analytical method that has been used to solve a variety of linear and non-linear dynamic or static problems in engineering especially for chain-type topology systems (i.e., pipes and its related elements); and, finally, hybrid techniques. The last one consists of combinations between the aforementioned methods, generally used to reduce the computational cost of FEM approaches or for a quick analysis of complicated piping systems, like the MOC-FEM [6] and the Finite Element Transfer Method (FETM) [10, 8, 13, 14] sometimes called as the Stiffness Matrix Method (SMM) [5], as well as others.

The emphasis of this work is to predict the structural harmonic response of pipeline systems subjected to internal "low-frequency" distributed loads (internal acoustic pulsation in frequencies equivalent to the first harmonics of typical compressors pulsation's spectra). It is assumed that the pipes are composed of linear elastic isotropic materials, for which the length is much larger than the diameter (at least 10 times) and the deflections are small compared to the pipe thickness. Under these hypotheses, this work does not consider high-order local deformation of the pipe wall: the objective is to analyze the global structural behavior of the pipeline system, which here is considered as a system of beams. Besides that, it is considered a "weak" coupling between structural and acoustic fields (one-way coupling) based on the resultant structural stresses over the pipe wall (obtained analytically from pipe section dimensions and internal pressure), which is converted in axial structural forces.

Also, it is assumed that there is an acoustic field through a non-dissipative ideal gas inside each pipe/duct, and that the structural vibration response of the pipe can be represented by the Timoshenko beam theory, for a defined domain and a set of boundary conditions. The problem is modeled by a combination of a TMM-based procedure (for acoustic field) and FEM (for structural field) considering reciprocating compressor pulsation as the main source of excitation under time-harmonic plane wave assumption. Here, the TMM-based procedure refers to the FETM, which can be implemented in the same way as FEM, enabling its application for complex geometries and facilitating the weak coupling procedure.

An open source code called *OpenPulse* was developed in Python to solve the AIV problem and, also, to solve separately the acoustic or the structural problem, when necessary. In this article, it is presented the main physical and numerical concepts that were used to develop *OpenPulse*, and the effectiveness of the adopted strategy is demonstrated using a simplified example application. The related engineering project is at an early stage, and we will present preliminary results without experimental validation.

2 Modelling the acoustic domain (1D acoustics)

Firstly, we need to model the acoustic domain inside the piping system. The main goal of the acoustic field analysis is the obtaining of the acoustic pressure (considering plane wave hypothesis) for a certain frequency range, at all points of a pipe system. After this procedure, the acoustic results are stored to be used in FEM structural analysis (Section 3) as a load case under certain coupling conditions (Section 4). In this section, the TMM formulation for an 1D hard-walled straight uniform duct element and its adaptation to FETM is briefly presented, including some considerations to obtain the global acoustic system.

2.1 Adapting Transfer Matrix Method (TMM) to Finite Element Transfer Method (FETM)

The TMM is a powerful mathematical technique to build discretized models for performing analytical and numerical studies of the plane wave acoustics in pipe systems. This method is particularly efficient to deal with plane acoustical waves in tubular circuits, because of the following aspects of the formulation [11]: (i) two scalar fields p and q are sufficient to describe the waves; (ii) use of exact analytical wave solutions for low order modes propagation (plane waves); (iii) only a few types of transfer matrices are necessary for assembling discretized tubular models; (iv) certain implementations and changes in boundary conditions (i.e., nodal impedances, position and kind of nodal sources) and extension to dissipative problems can be done maintaining the elementary formulation.

Consider a hard-walled straight uniform duct element as shown in Fig. 2. Gas properties like mean density ρ_f and speed of sound c_f are assumed to be uniform inside the tube. The volume velocity and pressure at the inlet of the element are denoted as q_1 and p_1, while q_2 and p_2 denote the corresponding quantities at the outlet. Z represents the acoustical impedance of the tube element. The objective is to find a matrix equation that expresses the volume velocity $q(x, k)$ and the pressure $p(x, k)$ at any point x inside the tube element at the wavenumber (frequency) $k = \omega/c_f$, in terms of their values at the inlet. Accordingly, the tube element can be represented as a matrix linear system with two inputs and two outputs as follows:

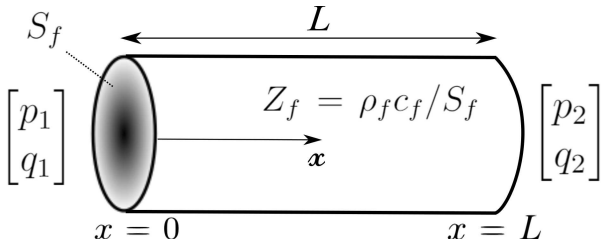

Figure 2: Uniform tube element (adapted from [11]).

$$\begin{bmatrix} p_2 \\ q_2 \end{bmatrix} = \mathbf{T}^e \begin{bmatrix} p_1 \\ q_1 \end{bmatrix}, \tag{1}$$

where $\mathbf{T}$ is the 2x2 transfer matrix for the uniform tube element.

To obtain each entry of $\mathbf{T}^e$, it is needed to solve the wave equation under the assumption of plane waves. By definition, the volume of fluid in a tube is characterized by one dimension, x, which is much larger than the others (the transverse dimensions). As a consequence, for a fluid oscillation at a given frequency ω, the compressibility parameter is predominant in the longitudinal direction. Moreover, if ω is small enough the compressibility parameter can be taken into account just in the longitudinal direction. So, the larger is the wavelength λ, the better the plane wave assumption works. Therefore, we can assume constant pressure in the hole tube cross-section and establish a frequency range validity for this assumption as

$$\frac{\lambda}{r_i} = \frac{c_f}{\omega r_i} >> 1, \tag{2}$$

where r_i is the inner duct radius. For this simple case, the homogeneous and non-dissipative wave equation is

$$p_{(xx)} - \frac{1}{c_f^2} p_{(tt)} = 0. \tag{3}$$

The sub-indexes inside parenthesis indicate derivatives.

Then, the 1D solution can be written in terms of traveling waves for the pressure as

$$p(x,t) = \left(A e^{-ikx} + B e^{ikx} \right) e^{i\omega t}. \tag{4}$$

Consequently, with the aid of Euler's equation:

$$q(x,t) = \frac{S_f}{\rho_f c_f} \left(A e^{-ikx} - B e^{ikx} \right) e^{i\omega t}, \tag{5}$$

where q is the interior volume velocity (which, for a given element n, is related to the particle velocity u_n by $q_n = S_{element_n} u_n$). From the mathematical standpoint, the two constants A and B appearing in the general solution of the local Eq. 3 are univocally defined if both the pressure and the volume velocity are specified at the inlet of the tube element.

Evaluating Eqs. 4 and 5 at $x = 0$ and $x = L$, the constants A and B are eliminated and the components of the transfer matrix $\mathbf{T}^e$ are obtained. Thus, Eq. 1 can be written as

$$\begin{bmatrix} p_2 \\ q_2 \end{bmatrix} = \begin{bmatrix} cos(kx) & -i\, Z_f\, sin(kx) \\ -\frac{i}{Z_f}\, sin(kx) & cos(kx) \end{bmatrix} \begin{bmatrix} p_1 \\ q_1 \end{bmatrix}, \tag{6}$$

where $Z_f = \rho_f c_f / S_f$ is the acoustic fluid impedance. Observe that $\mathbf{T}^e$ is not symmetric because of the choice made in the definition of the input and output vectors, which mix kinematics and stress variables (mixed formulation) [11].

To relate the TMM with a FEM-like matrix form, a few algebraic operations need to be done to rearrange the variables of the mixed formulation into one not mixed (the same type of variables in each nodal vector), which is more suitable with the FEM matrices. In structural mechanics, this method is known as FETM [10]. Taking the process suggested by [8] (one of the firsts that applied this procedure for duct acoustics), the TMM system of Eq. 6 can be adapted into the form (for a given duct element e)

$$\mathbf{K}_A^e \, \mathbf{p}^e = \mathbf{q}^e, \tag{7}$$

where $\mathbf{q}^e = [q_1, q_2]'$ and $\mathbf{p}^e = [p_1, p_2]'$ are the nodal volume velocities and the nodal pressures, respectively. $\mathbf{K}_A^e$ is the elementary matrix for a straight tube, which is presented in the expanded form of Eq. 7:

$$\begin{bmatrix} -i\,cot(kx)\,/\,Z_f & i\,/\,Z_f\,sin(kx) \\ i\,/\,Z_f\,sin(kx) & -i\,cot(kx)/\,Z_f \end{bmatrix} \begin{bmatrix} p_1 \\ p_2 \end{bmatrix} = \begin{bmatrix} q_1 \\ q_2 \end{bmatrix}. \tag{8}$$

The matrix $\mathbf{K}_A^e$ is known as the element Mobility Matrix [14], being clearly symmetric. This name probably is the most appropriated based on the mechanical/acoustic analogue force-velocity/pressure-volume velocity. $\mathbf{K}_A^e$ is also called Acoustic Stiffness Matrix [8], Admittance Matrix [15, 16] and Four-Pole Matrix [17]. In essence, the matrix $\mathbf{K}_A^e$ still depends on harmonically functions and on the fluid wave-number k, i.e., it is frequency dependent ($k = \omega/c_f$).

2.2 Obtaining the global acoustic Mobility Matrix

In order to obtain the global acoustic behavior of the system, the elementary matrices $\mathbf{K}_A^e$ are assembled respecting the connectivity of each pipe element. The global mobility matrix $\mathbf{K}_A$ is obtained doing the same procedure as adopted in FEM (see, e.g., [18]). In this work, each 1D acoustic element has two nodes and each node has 1 degree-of-freedom (DOF) (pressure). Also, the elements can have arbitrary length and cross-sectional area without harming the continuity of the field variables p and q. Briefly, the steps for the assembly process of the n $\mathbf{K}_A^e$ matrices, considering a system with n elements, are:

- node indexing in a convenient way (dependent on the desired bandwidth for $\mathbf{K}_A$);
- construction of the connectivity table;
- assembly of the n $\mathbf{K}_A^e$ matrices according to the connectivity table, leading to $\mathbf{K}_A$.

Thus, for a given excitation frequency ω, the global acoustic system is

$$\mathbf{K}_A \, \mathbf{p} = \mathbf{q}, \tag{9}$$

where $\mathbf{K}_A$ is the global Mobility Matrix, $\mathbf{p}$ are the nodal pressures and $\mathbf{q}$ are the nodal volume velocities for the whole system.

2.3 Acoustic boundary conditions (BC)

In the global system presented in Eq. 9, the global pressure vector $\mathbf{p}$ is presented as an unknown variable and must be found. Before solving the system, it is necessary to consider the applications of the BC's, which can be classified as:

- nodal volume velocity, q_i;
- nodal pressure, p_i;
- nodal acoustic impedance, Z_i, or element acoustic impedance, Z_{ij}. Some components like valves, cylinders, filters, etc, can be considered by their equivalent acoustic impedances.

These BC's can vary with the frequency. For example, one can consider to apply a table of pressure obtained from an experiment or to apply a table of acoustic impedance that represents a valve, etc. More details on the implementation of BC's used in this work can be found in [19].

2.4 Some other characteristics considered in the implementation of acoustics in *OpenPulse*

Some features also implemented in *OpenPulse* that are detailed in [19]:

- capability of considering a mean flow velocity;
- adjust of effective element lengths depending on the transition of pipe diameters (e.g., in expansion chambers and side branches);
- materials properties related to specific regions, making it possible to change gas properties according to the operational characteristics of each region of the domain (temperature, mean pressure, etc);
- addition of dissipation through inserting a complex wave number $\overline{k}$, if needed.

3 Modelling the structural domain (3D Timoshenko beam)

Once the acoustic domain is modeled, now we need to describe the structural part of the system. Structural FEM models based on beam theory are well consolidated for predicting global vibrations of pipe systems (considering here that the length of the pipes is much larger than the diameter, with small deflections and global behavior). The classical Euler-Bernoulli beam theory requires C^1-continuity, resulting in schemes that can be complicated to be implemented for multidimensional problems. On the other hand, the classical Timoshenko beam theory requires only C^0-continuity, enabling the use of finite element shape functions that are easily constructed. The C^0 Timoshenko's formulation also allows us to obtain better stress/strain values when compared to other procedures.

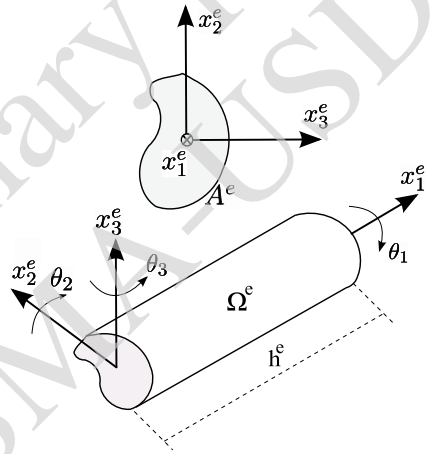

Figure 3: 3D beam local coordinates.

3.1 Main assumptions

It is initially assumed that the $\{x_1^e, x_2^e, x_3^e\}$-axes are locally defined at the centroid of the beam segment cross-section and are principal axes [18], as can be seen in Fig. 3. A more detailed assumption is considered in *OpenPulse* [19], but the present one is sufficient to explain the structural modelling without losing of physical meaning.

The tridimensional displacements of a point (x_1, x_2, x_3) that belongs to a cross-sectional area A^e placed in x_1 are given by [20, 18, 21]:

$$u_1(x_1, x_2, x_3, t) = w_1(x_1, t) - x_2\theta_3(x_1, t) + x_3\theta_2(x_1, t), \tag{10}$$

$$u_2(x_1, x_2, x_3, t) = w_2(x_1, t) - x_3\theta_1(x_1, t), \tag{11}$$

$$u_3(x_1, x_2, x_3, t) = w_3(x_1, t) + x_2\theta_1(x_1, t). \tag{12}$$

Consequently, the movement of a given point (x_1, x_2, x_3) in the element domain Ω^e is described by $\boldsymbol{u}(x_1, x_2, x_3, t) = [u_1, u_2, u_3]$.

The translation components w_i of the neutral line and the rotation angles θ_i of the sectional area are illustrated in Fig. 4. These kinematic constraints do not include warping (the plane sections remain plane). Besides that, it is considered that w_1, w_2 and w_3 are small when compared to h^e, and $\sin\theta_i \approx \tan\theta_i \approx \theta_i$.

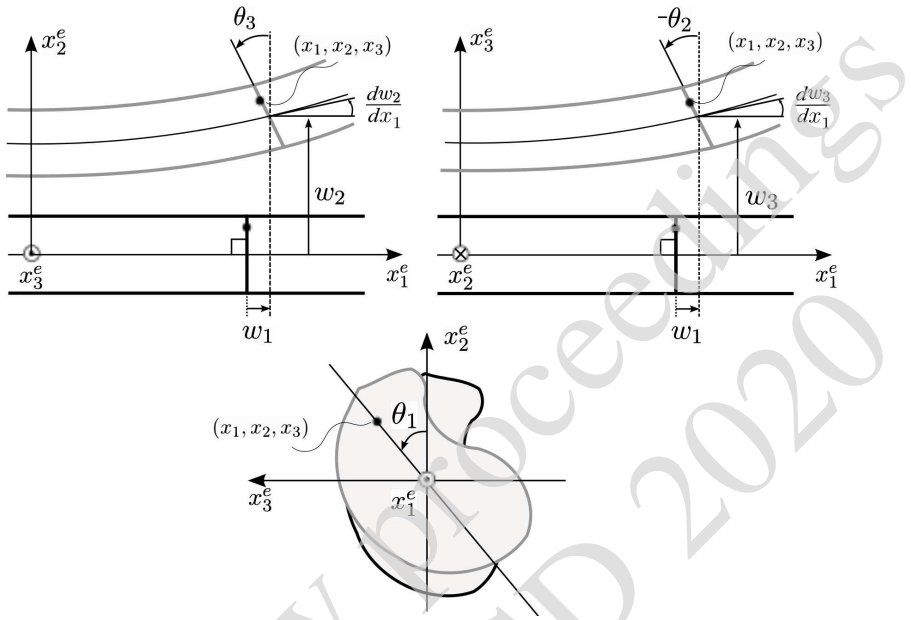

Figure 4: Deformation components in Timoshenko beam theory.

Different from Euler-Bernoulli theory, here σ_{21} $(= \sigma_{12})$ and σ_{31} $(= \sigma_{13})$ are not null (shear stress is considered). However, $\sigma_{23} = 0$ and $\sigma_{32} = 0$ (there is no bending along x_2 and x_3). Considering the homogeneous isotropic case, we have [18]:

$$\sigma_{ij} = \lambda\epsilon_{kk}\delta_{ij} + 2\mu\epsilon_{ij}, \tag{13}$$

where δ_{ij} is the "delta of Kronecker" (see [22] for a review on continuum mechanics), and λ and μ are the Lamé parameters, which are obtained by:

$$\lambda = \frac{\nu E}{(1+\nu)(1-2\nu)}, \qquad \mu = \frac{E}{2(1+\nu)}. \tag{14}$$

The Young's modulus E and the Poisson's ratio ν are intrinsic material properties considering an isotropic media. Assuming the hypothesis for shear previously presented and Eq. 13, the following constitutive relations are obtained:

$$\sigma_{11} = E\epsilon_{11}, \qquad \sigma_{\gamma 1} = 2\mu\epsilon_{\gamma 1}, \tag{15}$$

and with $\gamma = 2, 3$.

From Eqs. 10 to 12, the kinematic relations (strain-displacement equations) can be obtained as follows:

$$\epsilon_{\beta\gamma} = u_{(\beta\gamma)} = 0, \tag{16}$$

$$\epsilon_{11} = w_1' - x_2\theta_3' + x_3\theta_2', \tag{17}$$

$$\epsilon_{21} = \frac{1}{2}(w_2' - x_3\theta_1' - \theta_3), \tag{18}$$

$$\epsilon_{31} = \frac{1}{2}(w_3' + x_2\theta_1' + \theta_2). \tag{19}$$

where the primes denote differentiation with respect to x_1 ($d(\cdot)/dx_1$), and $\beta\gamma = 23, 32$.

3.2 Mechanical equilibrium and variational equation

Assuming the local condition of mechanical equilibrium in a continuum medium Ω, and considering the virtual displacement field $\overline{\boldsymbol{u}}$ (a kinematic admissible field), the variational equation can be written as [18, 21]:

$$\int_\Omega \overline{u}_{(ij)}\sigma_{ij}d\Omega - \int_\Omega \overline{u}_i F_i d\Omega - \int_{\Gamma_k} \overline{u}_i k_i d\Gamma + \int_\Omega \overline{u}_i \rho \ddot{u}_i d\Omega = 0, \tag{20}$$

where Γ_g is the boundary of Ω where Dirichlet boundary conditions g_i are applied, and Γ_k is the boundary of Ω where Newmann boundary conditions k_i are applied (at normal direction n). The entity $\boldsymbol{F}$ represents the body forces acting on Ω and ρ is the density of the material. The sub-indexes inside parenthesis indicate derivatives.

Considering $dA = dx_2dx_3$, the domain can be represented by elements as follows:

$$\int_\Omega d\Omega = \sum_{e=1}^{nel}\int_{\Omega_e} d\Omega = \sum_{e=1}^{nel}\int_0^{h_e}\int_{A^e} dAdx_1. \tag{21}$$

Assuming $\Gamma_k = \{\oslash\}$ due to the "line shape" of the simplified structure [18], it is applied the hypothesis that all distributed external loads (force/length or moment/length) can be considered in the body force vector $\boldsymbol{F}$. By this way, Eq. 20 can be rewritten as

$$\begin{aligned} 0 = \sum_{e=1}^{nel}\Bigg\{ & \int_0^{h_e}\Big(\overline{\gamma}_2\mu A_s^e\gamma_2 + \overline{\gamma}_3\mu A_s^e\gamma_3 + \overline{\kappa}_2 EI_2^e\kappa_2 + \overline{\kappa}_3 EI_3^e\kappa_3 + \overline{\epsilon}EA^e\epsilon + \overline{\Psi}\mu J^e\Psi\Big)dx_1 \\ & - \int_0^{h_e}\Big(\overline{w}_2F_2 + \overline{w}_3F_3 + \overline{w}_1F_1 + \overline{\theta}_2C_2 - \overline{\theta}_3C_3 + \overline{\theta}_1C_1\Big)dx_1 \\ & + \int_0^{h_e}\Big((\overline{w}_2\ddot{w}_2 + \overline{w}_3\ddot{w}_3 + \overline{w}_1\ddot{w}_1)\rho A^e + \overline{\theta}_1\ddot{\theta}_1\rho J^e + \overline{\theta}_2\ddot{\theta}_2\rho I_2^e + \overline{\theta}_3\ddot{\theta}_3\rho I_3^e\Big)dx_1\Bigg\}, \end{aligned} \tag{22}$$

or, using a matricial form (and now emphasizing that the integration is performed over the element length):

$$\begin{aligned} 0 = \sum_{e=1}^{nel}\Bigg\{ & \int_0^{h_e}\Big[\overline{\boldsymbol{\gamma}}^T\mathbf{D}^s\boldsymbol{\gamma} + \overline{\boldsymbol{\kappa}}^T\mathbf{D}^b\boldsymbol{\kappa} + \overline{\epsilon}(EA^e)\epsilon + \overline{\Psi}(\mu J^e)\Psi\Big]dx_1^e \\ & - \int_0^{h_e}\Big[\overline{\boldsymbol{w}}^T\boldsymbol{F} + \overline{\boldsymbol{\theta}}^T\boldsymbol{C}\Big]dx_1^e + \int_0^{h_e}\Big[\overline{\boldsymbol{w}}^T\mathbf{G}^{tr}\ddot{\boldsymbol{w}} + \overline{\boldsymbol{\theta}}^T\mathbf{G}^r\ddot{\boldsymbol{\theta}}\Big]dx_1^e\Bigg\}, \end{aligned} \tag{23}$$

where [18]

$$\boldsymbol{w} = \begin{bmatrix} w_1 \\ w_2 \\ w_3 \end{bmatrix}, \boldsymbol{\theta} = \begin{bmatrix} \theta_1 \\ \theta_2 \\ \theta_3 \end{bmatrix}, \boldsymbol{\gamma} = \begin{bmatrix} \gamma_2 \\ \gamma_3 \end{bmatrix}, \boldsymbol{\kappa} = \begin{bmatrix} \kappa_2 \\ \kappa_3 \end{bmatrix}, \tag{24}$$

$$\mathbf{D}^s = \begin{bmatrix} \mu A_s^e & 0 \\ 0 & \mu A_s^e \end{bmatrix}, \mathbf{D}^b = \begin{bmatrix} EI_2^e & 0 \\ 0 & EI_3^e \end{bmatrix}, \tag{25}$$

$$\mathbf{G}^{tr} = \begin{bmatrix} \rho A^e & 0 & 0 \\ 0 & \rho A^e & 0 \\ 0 & 0 & \rho A^e \end{bmatrix}, \mathbf{G}^{r} = \begin{bmatrix} \rho J^e & 0 & 0 \\ 0 & \rho I_2^e & 0 \\ 0 & 0 & \rho I_3^e \end{bmatrix}, \tag{26}$$

and: $\Psi = \theta_3'$; $\kappa_\beta = \theta_\beta'$ is called "curvature"; $\epsilon = w_1'$; $\gamma_2 = w_2' - \theta_3$; $\gamma_3 = w_3' + \theta_2$; $F_i = \{F_i^e\}$ and $C_i = \{C_i^e\}$ are the element applied external forces and couples, respectively, per unity length, for $1 \leq e \leq nel$. In this text, in order to simplify the presentation of the main hypotheses, the assumption that $\{x_1^e, x_2^e, x_3^e\}$-axes are locally defined at the centroid of the beam segment cross-section (and that they are principal axes) decouples bending from axial strain, in addition to decoupling torsional from transversal strain. In *OpenPulse*, a more real assumption is considered (see [19]).

In the above equations, J^e, I_2^e and I_3^e are the area moments of inertia and A_s^e is the effective shear area considering a representative shear correction factor [23].

3.3 Structural Finite Element Method

The FEM procedure is implemented assuming that [18]:

$$w_i^e(x_1, x_2, x_3, t) = \sum_{a=1}^{npel} \mathrm{N}_a \mathrm{w}_{ia}^e, \quad \text{and} \quad \theta_i^e(x_1, x_2, x_3, t) = \sum_{a=1}^{npel} \mathrm{N}_a \theta_{ia}^e, \tag{27}$$

where N_a is the shape function related to the "weights" w_{ia} and θ_{ia} at node a in element e.

In order to obtain the element matrices, we assume the following vector form for the element's degrees of freedom weights and element's load weights: $\mathbf{d}^e = [\mathrm{w}_{11}^e, \mathrm{w}_{21}^e, \mathrm{w}_{31}^e, \theta_{11}^e, \theta_{21}^e, \theta_{31}^e, \ldots, \mathrm{w}_{1npel}^e, \mathrm{w}_{2npel}^e, \mathrm{w}_{3npel}^e, \theta_{1npel}^e, \theta_{2npel}^e, \theta_{3npel}^e]'$. Consequently,

$$\begin{bmatrix} w_1^e(x_1, x_2, x_3, t) \\ w_2^e(x_1, x_2, x_3, t) \\ w_3^e(x_1, x_2, x_3, t) \\ \theta_1^e(x_1, x_2, x_3, t) \\ \theta_2^e(x_1, x_2, x_3, t) \\ \theta_3^e(x_1, x_2, x_3, t) \end{bmatrix} = \mathbf{N}\mathbf{d}^e, \tag{28}$$

where $\mathbf{N}$ is the matrix of shape functions. Considering $\mathbf{B}^a$, $\mathbf{B}^b$, $\mathbf{B}^s$ and $\mathbf{B}^s$ the matrices of shape functions derivatives depending on the strain evaluated in Eq. 23, the element stiffness matrix $\mathbf{K}^e$ is obtained as [18]

$$\mathbf{K}^e = \mathbf{K}_b^e + \mathbf{K}_s^e + \mathbf{K}_a^e + \mathbf{K}_t^e, \tag{29}$$

$$\mathbf{K}_b^e = \int_0^{h_e} \mathbf{B}^{bT} \mathbf{D}^b \mathbf{B}^b dx_1^e \text{ (bending stiffness)}, \quad \mathbf{K}_s^e = \int_0^{h_e} \mathbf{B}^{sT} \mathbf{D}^s \mathbf{B}^s dx_1^e \text{ (shear stiffness)}, \tag{30}$$

$$\mathbf{K}_a^e = \int_0^{h_e} \mathbf{B}^{aT} (EA) \mathbf{B}^a dx_1^e \text{ (axial stiffness)}, \quad \mathbf{K}_t^e = \int_0^{h_e} \mathbf{B}^{tT} (\mu J) \mathbf{B}^t dx_1^e \text{ (torsional stiffness)}. \tag{31}$$

The element mass matrix $\mathbf{M}^e$ is obtained as

$$\mathbf{M}^e = \mathbf{M}_{tr}^e + \mathbf{M}_r^e, \tag{32}$$

$$\mathbf{M}_{tr}^e = \int_0^{h_e} \mathbf{N}^{trT} \mathbf{G}^{tr} \mathbf{N}^{tr} dx_1^e \text{ (translational mass)}, \quad \mathbf{M}_r^e = \int_0^{h_e} \mathbf{N}^{rT} \mathbf{G}^{r} \mathbf{N}^{r} dx_1^e \text{ (rotational mass)}. \tag{33}$$

Considering $\mathbf{F}_{intg} = [F_1, F_2, F_3, C_1, C_2, C_3]'$, the element force vector is obtained as follows:

$$\mathbf{f}^e = \int_0^{h_e} \mathbf{N}^T \mathbf{F}_{intg} dx_1^e. \tag{34}$$

3.4 Obtaining the global structural system of equations

To obtain the global structural behavior of the system, the elementary entities $\mathbf{K}_e$, $\mathbf{M}_e$ and $\mathbf{p}_e$ are assembled, after local to global coordinate system transformation [21], respecting the connectivity of each beam element. The elements can have arbitrary length and cross-sectional area without harming the continuity of the field variables. After the assembling procedure, the global structural system is

$$\mathbf{K}\mathbf{d} + \mathbf{M}\ddot{\mathbf{d}} = \mathbf{f}, \tag{35}$$

where $\mathbf{K}$ and $\mathbf{M}$ are global stiffness and mass matrices, respectively, $\mathbf{d}$ are the nodal displacements and rotations, and $\mathbf{f}$ are the nodal forces and moments for the whole system. In this work, the objective is to analyze time-harmonic vibrations. So, the system above can be rewritten as

$$\big(\mathbf{K} - \omega^2\mathbf{M}\big)\mathbf{d}(\omega) = \mathbf{f}(\omega). \tag{36}$$

3.5 Damping model

The damping matrix $\mathbf{C}$ used in harmonic analysis (considering only the material damping) is defined as

$$\mathbf{C} = \alpha\mathbf{M} + (\beta + \frac{1}{\omega}\eta)\mathbf{K}, \tag{37}$$

where α is the mass-proportional coefficient, β is stiffness-proportional coefficient, and η is the structural (hysteretic) damping. $\omega = 2\pi f$, where f is the excitation frequency. Eq. 36 is rewritten as

$$\big(\mathbf{K} + j\omega\mathbf{C} - \omega^2\mathbf{M}\big)\mathbf{d}(\omega) = \mathbf{f}(\omega). \tag{38}$$

3.6 Structural boundary conditions (BC)

In the global system presented in Eq. 35, the global vector $\mathbf{d}$ is presented as an unknown variable and must be found. Before solving the system, it is necessary to consider the applications of the BC's, which can be classified as:

- nodal forces and/or moments, f_i;
- nodal displacements and/rotations, d_i;
- nodal lumped parameters: mass, spring and dampers.

These BC's can vary with the frequency. For example, one can consider to apply a table of accelerations obtained from an experiment, or to apply a table of spring stiffness that represents supports, etc. More details on the implementation of BC's used in this work can be found in [19].

3.7 Some other characteristics considered in the implementation of beams in *OpenPulse*

Some features also implemented in *OpenPulse* that are detailed in [19]:

- possibility of applying an offset between local coordinates and the beam's neutral axis as described in [24].
- calculation of section properties and shear correction factor through a FE mesh of each section, as described in [24].
- different materials can be associated to different regions, making it possible to change pipe properties according to the operational/structural characteristics of each part of the domain;
- addition of distributed mass for representing insulation material, if relevant.

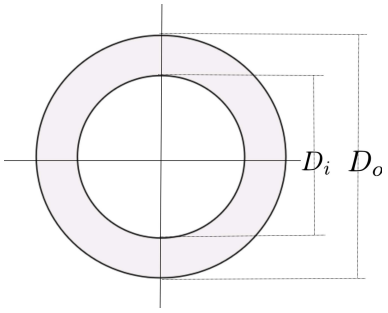

Figure 5: Section of the pipe element.

4 Acoustic-structure one-way coupling

In the previous section, the acoustic behavior of the fluid being transported throughout pipes and the structural behavior of pipeline systems were described independently (by assuming appropriate hypotheses that allow modeling each behavior independently). However, the objective of this work is to predict the dynamic response of structural systems subjected to harmonic acoustic loads.

In this research, we consider the structural pipe element as a beam with a hollow section, as can be seen in Fig. 5. The acoustic pipe element is configured in such a manner that the FETM mesh is the same as that used for FEM structural analysis. Additionally, the acoustic pipe element diameter equals to the internal structural diameter D_i considered in the respective beam element.

There are some important works on the formulation of an "elasto-acoustic" beam based on the "strong" coupling between structural and fluid fields [25, 26, 27, 28]. However, in this work it is assumed a "weak" coupling (one-way coupling) based on the following hypotheses:

- the fluid is a gas;
- the viscosity of the fluid is negligible;
- the acoustic plane wave propagates in axial direction (1-D acoustics);
- the pipe is thin-walled and linearly elastic;
- the radial inertia of the pipe wall is neglected if considering low frequencies ($ka << 1$) [29];
- the acoustic wave speed c_f in the gas is affected by the mechanical compliance of the pipe wall [29] and is given by:

$$c_f = \left(\frac{\rho_f}{K_f} \left(1 + \frac{D_i K_f}{Et} \right) \right)^{-1/2}, \tag{39}$$

  where ρ_f is the fluid mass density, K_f is the fluid bulk modulus, E is the Young's modulus of pipe material, D_i is the internal diameter and t is the pipe wall thickness;

- resultant normal and shear stresses in the structure are derived from the internal fluid pressure under the assumptions: i) plane stress conditions in the wall; ii) cross sections remain plane to the neutral axis.

4.1 Internal pressure effect on a structural pipe: equivalent load vector

The internal pressure has a zero external resultant force acting on the pipe. However, in the approach used in this work [30, 31], considering the assumptions listed above, the load equivalent to the stress field induced by the pressure effect is applied on each element as an external axial load, considering harmonic pulsation/vibration with an excitation frequency ω.

The axial stress is resultant from the difference between internal and external pressure, and is given by

[32, 30]:

$$\sigma_1(\omega) = \frac{p_i(\omega)D_i^2 - p_o D_o^2}{D_o^2 - D_i^2}, \tag{40}$$

where $p_i(\omega)$ is the internal pressure, obtained from the acoustic problem defined in Eq. 9 considering Eq. 39; D_i is the internal diameter; D_o is the external diameter; and p_o is the external pressure, considered constant in this work.

The radial stress can be obtained using the Lamé stress distribution [32, 30], using the internal and external pressures as a boundary condition:

$$\sigma_r(r,\omega) = \frac{p_i(\omega)D_i^2 - p_o D_o^2}{D_o^2 - D_i^2} - \frac{D_i^2 D_o^2 (p_i(\omega) - p_o)}{4r^2(D_o^2 - D_i^2)}. \tag{41}$$

And the hoop (circumferential) stress is obtained using the same stress distribution considered in the radial case, resulting in:

$$\sigma_c(r,\omega) = \frac{p_i(\omega)D_i^2 - p_o D_o^2}{D_o^2 - D_i^2} + \frac{D_i^2 D_o^2 (p_i(\omega) - p_o)}{4r^2(D_o^2 - D_i^2)}. \tag{42}$$

Consequently, the axial equivalent forces acting at both ends of each element can be found, and the additional element load vector $\mathbf{f}_p^e$, which must be added to Eq. 34, is given by:

$$\mathbf{f}_p^e = \begin{bmatrix} F_p, 0, 0, 0, 0, 0, -F_p, 0, 0, 0, 0, 0 \end{bmatrix}', \tag{43}$$

where

$$F_p = A_e E \left[\frac{1}{E} \left(\sigma_1 - \nu(\sigma_r + \sigma_c) \right) \right]. \tag{44}$$

After this procedure, the new element load vectors $\mathbf{f}_p^e$ can be assembled and added to the global vector $\mathbf{f}$, which allows the calculation of the displacements vector $\mathbf{d}$ through Eq. 38. The axial stress σ_1 is considered only in the "capped end" condition [19].

4.2 Fluid mass effect

The mass of the gas is considered distributed throughout the length of the structural elements. Thus, the matrix $\mathbf{G}^{tr}$ in Eq. 26 is modified as follows

$$\mathbf{G}^{tr\prime} = \mathbf{G}^{tr} + \begin{bmatrix} \rho_f A_i & 0 & 0 \\ 0 & \rho_f A_i & 0 \\ 0 & 0 & \rho_f A_i \end{bmatrix}, \tag{45}$$

where A_i is the internal area of the pipe, calculated with D_i.

5 Implementation and user interface using Python

OpenPulse is a open-source software written in Python 3.7.7, with the requirement of installing the libraries numpy, scipy, vtk, PyQt5 and matplotlib. The software is implemented in a way that follows the sequence illustrated in Fig. 6.

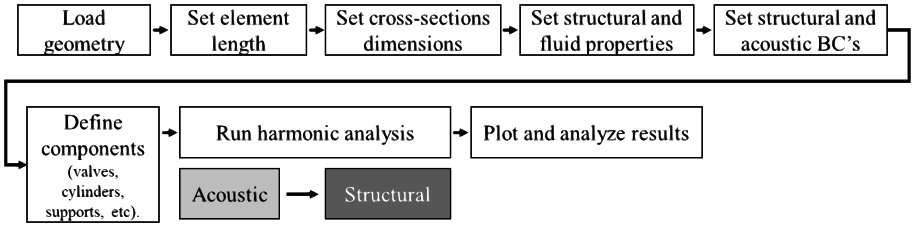

Figure 6: Sequence of problem set-up in *OpenPulse*.

A friendly interface allows the user to import the geometry of the pipe system (lines in IGES format), insert materials properties, set sections, and import pressure/acceleration/force loads (from measurements or theory), as can be seen in Figs. 7 and 8. After defining the FEM mesh for the model, the user can plot the piping system geometry, see the FE mesh, and run the desired simulations after a proper setup. It is possible to plot deformed shapes, frequency plots of acoustical and structural responses, stress fields, and local stresses of desired sections.

The code and a more detailed description of the implementation can be found in [19].

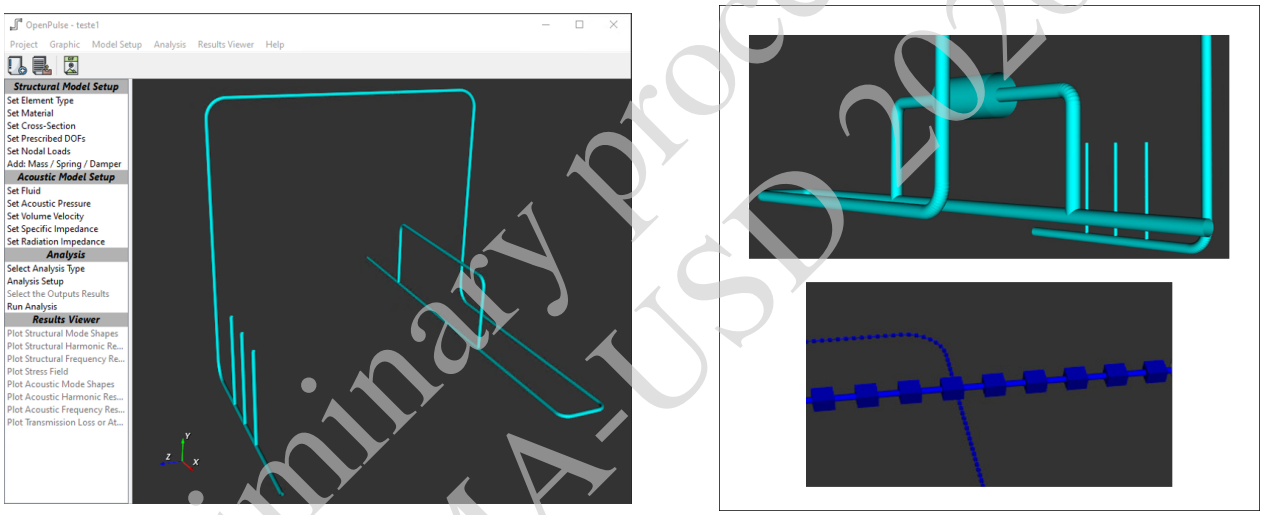

(a) (b)

Figure 7: (a) Main window of *OpenPulse*. View of imported IGES (lines). (b) Details of geometry (after setting sections) and FE mesh.

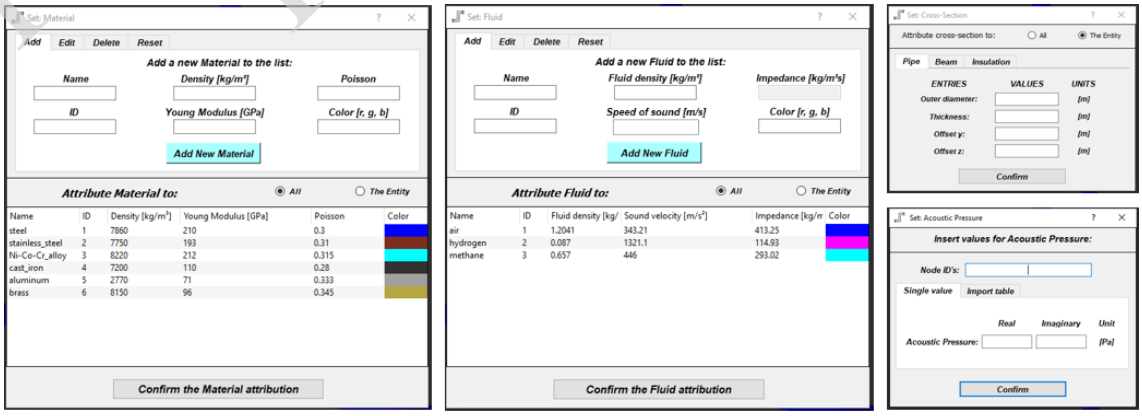

Figure 8: Entry of properties, section parameters and loads in *OpenPulse*.

6 Simplified example of application

In this section, the simplified piping system presented in Fig. 7 is analyzed. The maximum pipe length in the model is 2.25 m. The element size for acoustic and structural analyses is 0.01 m (the same mesh is used in both analyses). The external and internal diameters are D_o = 0.05 m and D_i = 0.034 m. An expansion chamber is considered (see Fig. 7b) with D_o = 0.2 m and D_i = 0.184 m. Three identical capped end branches (see Fig. 7a and 7b) are set with D_o = 0.025 m and D_i = 0.017 m. The structure is modelled considering steel pipes with $E = 210$ GPa, ν = 0.3 and ρ = 7860 kg/m^3. The gas being transported is hydrogen with ρ_f = 0.087 kg/m^3 and c_f = 1321.1 m/s. In this simple example, no dissipation or damping is considered.

In this example, it is considered an acoustic BC equivalent to a compressor pulsation (simplified) in the discharge. A table with the frequency spectrum of the pressure is imported and applied as a pressure BC. This simplified spectrum of excitation can be seen in Fig. 9a. Acoustic impedance is applied as indicated in Fig. 9b to simulate an infinite tube. For the structure, it is considered a fixation of all translational movements (rotations free) in the nodes marked in Figure 9b. Remembering that it is possible to set other boundary conditions for structural analysis as forces, vibrations, springs, etc.

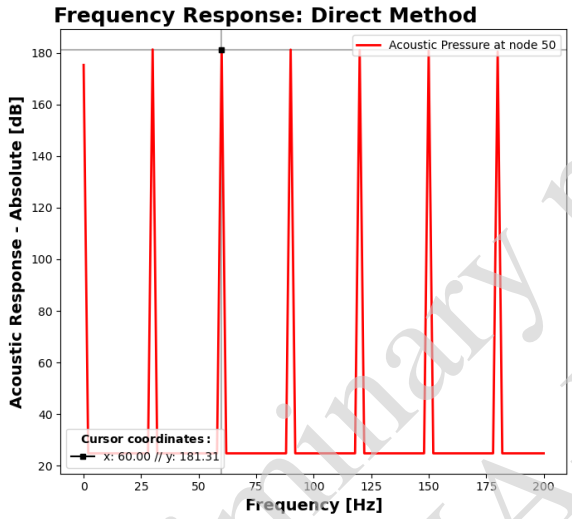

(a)

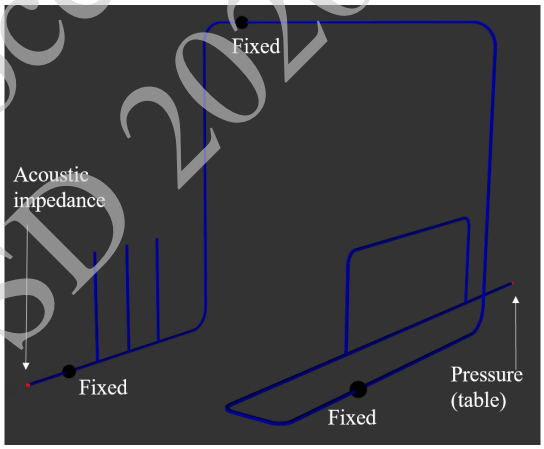

(b)

Figure 9: (a) Frequency plot of imported pressure. (b) Acoustic and structural BCs (presentation in FE mesh view).

According to the imported pressure table, the harmonic analysis is set to run from 0 to 200 Hz, with increments of 2 Hz. The acoustic and structural responses of the piping system are presented in Fig. 10 for an excitation frequency of 60 Hz (second harmonic in the spectrum of the excitation pressure).

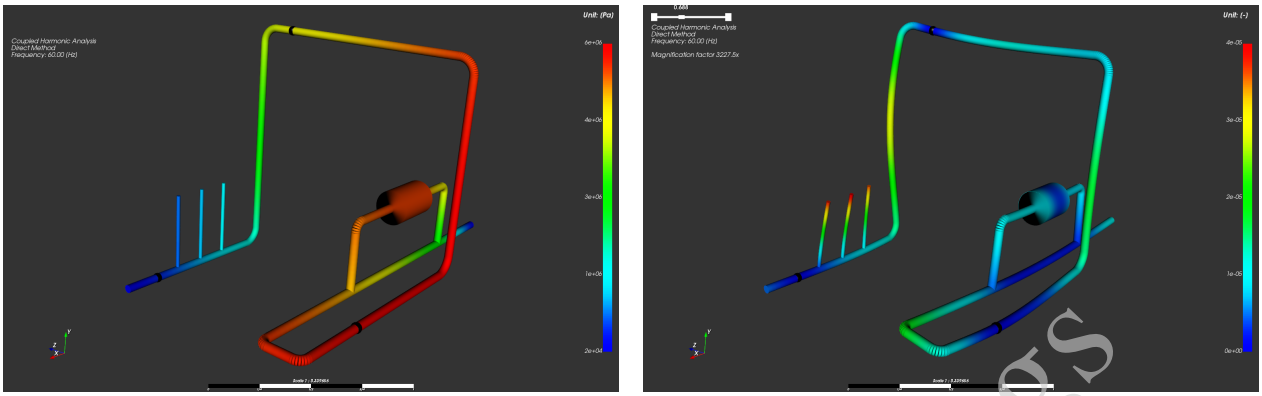

(a) (b)

Figure 10: (a) Acoustic response and (b) structural response at 60 Hz. Colormap: amplitudes.

The frequency plot of acoustic pressure and structural displacement can be done in the results module of *OpenPulse*. For example, a node at the left largest vertical tube (node 561) is analyzed in Fig. 11.

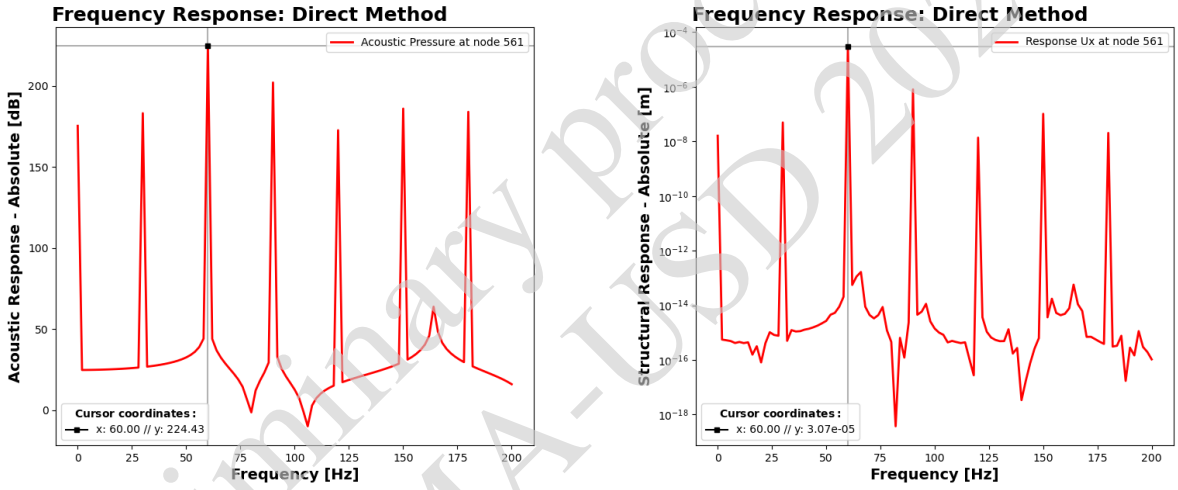

(a) (b)

Figure 11: (a) Frequency plot of pressure amplitude and (b) x-displacement amplitude at node 561.

7 Conclusions

In this work, the authors presented physical and numeric details of the implementation of an open source software - the *OpenPulse* - with the objective of analyzing acoustically induced vibration caused in pipeline systems by low-frequency internal pulsation. The related project is in an early stage, but the first results present coherent significance, which can be validated with other commercial FEM codes (using 3D FEM acoustic analysis and 3D beam structures). The authors hope to publish a future work presenting the different possibilities of using *OpenPulse* in more realistic examples, considering more piping elements (valves, chambers, etc) and comparing them with experimental results.

Acknowledgements

We acknowledge that *OpenPulse* development is supported by Petrobras, Universidade Federal de Santa Catarina (UFSC) and Agência Nacional de Petróleo, Gás Natural e Biocombustíveis (ANP).

References

[1] N. I. do Brasil, M. A. S. Araujo, and E. C. M. Sousa, *Processamento de Petroleo e Gas (Portuguese)*. Rio de Janeiro, Brazil: LTC, 2014.

[2] J. Fink, "Chapter 10 - special refinery additives," in *Guide to the Practical Use of Chemicals in Refineries and Pipelines*, J. Fink, Ed. Boston: Gulf Professional Publishing, 2016, pp. 173 – 183.

[3] R. A. Parisher and R. A. Rhea, *Pipe Drafting and Design*. Gulf Professional Publishing, 2012. [Online]. Available: https://www.sciencedirect.com/book/9780123847003

[4] "Chapter 1 - introduction," in *Flow-induced Vibrations (Second Edition)*, second edition ed., S. Kaneko, T. Nakamura, F. Inada, M. Kato, K. Ishihara, T. Nishihara, and M. A. Langthjem, Eds. Oxford: Academic Press, 2014, pp. 1 – 28. [Online]. Available: http://www.sciencedirect.com/science/article/pii/B9780080983479000011

[5] "Chapter 5 - vibration induced by pressure waves in piping," in *Flow-induced Vibrations (Second Edition)*, second edition ed., S. Kaneko, T. Nakamura, F. Inada, M. Kato, K. Ishihara, T. Nishihara, and M. A. Langthjem, Eds. Oxford: Academic Press, 2014, pp. 197 – 275. [Online]. Available: http://www.sciencedirect.com/science/article/pii/B9780080983479000059

[6] S. Li, B. W. Karney, and G. Liu, "Fsi research in pipeline systems – a review of the literature," *Journal of Fluids and Structures*, vol. 57, pp. 277 – 297, 2015. [Online]. Available: http://www.sciencedirect.com/science/article/pii/S0889974615001590

[7] A. Coulon, R. Salanon, and L. Ancian, "Innovative numerical fatigue methodology for piping systems: qualifying acoustic induced vibration in the oil&gas industry," *Procedia Engineering*, vol. 213, pp. 762 – 775, 2018, 7th International Conference on Fatigue Design, Fatigue Design 2017, 29-30 November 2017, Senlis, France.

[8] A. Craggs, "The application of the transfer matrix and matrix condensation methods with finite elements to duct acoustics," *Journal of Sound and Vibration*, vol. 132, no. 3, pp. 393 – 402, 1989. [Online]. Available: http://www.sciencedirect.com/science/article/pii/0022460X89906330

[9] A. Sahasrabudhe, S. Ramu, and M. Munjal, "Matrix condensation and transfer matrix techniques in the 3-d analysis of expansion chamber mufflers," *Journal of Sound and Vibration*, vol. 147, no. 3, pp. 371 – 394, 1991. [Online]. Available: http://www.sciencedirect.com/science/article/pii/0022460X91904875

[10] A. Tesár and L. Fillo, *Transfer matrix method*, ser. Mathematics and its applications (Kluwer Academic Publishers).: East European series. Kluwer Academic Publishers, 1988. [Online]. Available: https://books.google.com.br/books?id=qc5RAAAAMAAJ

[11] "Chapter 4 plane acoustical waves in pipe systems," in *Fluid-Structure Interaction*, ser. Modelling of Mechanical Systems, F. Axisa and J. Antunes, Eds. Butterworth-Heinemann, 2007, vol. 3, pp. 243 – 352. [Online]. Available: http://www.sciencedirect.com/science/article/pii/S1874705107800077

[12] K. Botros and T. Van Hardeveld, *Pipeline Pumping and Compression Systems: A Practical Approach*. ASME Press, 2018. [Online]. Available: https://books.google.com.br/books?id=8nFluQEACAAJ

[13] A. Craggs and D. C. Stredulinsky, "Analysis of acoustic wave transmission in a piping network," *The Journal of the Acoustical Society of America*, vol. 88, no. 1, pp. 542–547, 1990. [Online]. Available: https://doi.org/10.1121/1.399935

[14] A. Frid, "Fluid vibration in piping systems—a structural mechanics approach, i: Theory," *Journal of Sound and Vibration*, vol. 133, no. 3, pp. 423 – 438, 1989. [Online]. Available: http://www.sciencedirect.com/science/article/pii/0022460X89906081

[15] F. Chevillotte and R. Panneton, "Coupling transfer matrix method to finite element method for analyzing the acoustics of complex hollow body networks," *Applied Acoustics*, vol. 72, no. 12, pp. 962 – 968, 2011. [Online]. Available: http://www.sciencedirect.com/science/article/pii/S0003682X11001708

[16] M. Nijhof, "Viscothermal wave propagation," Ph.D. dissertation, University of Twente, Netherlands, 12 2010.

[17] C. To, "The acoustic simulation and analysis of complicated reciprocating compressor piping systems, i: Analysis technique and parameter matrices of acoustic elements," *Journal of Sound and Vibration*, vol. 96, no. 2, pp. 175 – 194, 1984. [Online]. Available: http://www.sciencedirect.com/science/article/pii/0022460X84905777

[18] T. Hughes, *The Finite Element Method: Linear Static and Dynamic Finite Element Analysis*, ser. Dover Civil and Mechanical Engineering. Dover Publications, 2000. [Online]. Available: https://books.google.com.br/books?id=yarmSc7ULRsC

[19] MOPT, "Open pulse: Open source software for pulsation analysis of pipeline systems." [Online]. Available: https://open-pulse.github.io/openpulse/

[20] L. Andersen and S. R. K. Nielsen, *Elastic Beams in Three Dimensions*. DCE Lecture Notes No. 23 - Aalborg University, 2008. [Online]. Available: http://homes.civil.aau.dk/jc/FemteSemester/Beams3D.pdf

[21] O. C. Zienkiewicz and R. L. Taylor, *The Finite Element Method For Solid and Structural Mechanics*. Butterworth-Heinemann, 2005.

[22] G. A. Holzapfel, *Nonlinear Solid Mechanics: A Continuum Approach for Engineering*. Wiley, 2000.

[23] E. Oñate, *Structural Analysis with the Finite Element Method. Linear Statics. Volume 2: Beams, Plates and Shells*. CIMNE, 2013.

[24] W. D. Pilkey, *Anslysis and Desing of Elastic Beams: Computational Methods*. John Wiley & Sons, Inc., 2002.

[25] R. Ohayon, "Variational analysis of a slender fluid–structure system: The elasto-acoustic beam—a new symmetric formulation," *International Journal for Numerical Methods in Engineering*, vol. 22, no. 3, pp. 637–647, 1986.

[26] N. Piet-Lahanier and R. Ohayon, "Finite element analysis of a slender fluid—structure system," *Journal of Fluids and Structures*, vol. 4, no. 6, pp. 631 – 645, 1990.

[27] A. Tijsseling, "Fluid-structure interaction in liquid-filled pipe systems: A review," *Journal of Fluids and Structures*, vol. 10, no. 2, pp. 109 – 146, 1996.

[28] D. Ferras, P. A. Manso, A. J. Schleiss, and D. I. C. Covas, "One-dimensional fluid–structure interaction models in pressurized fluid-filled pipes: A review," *Applied Sciences*, vol. 8, no. 10, 2018.

[29] T. C. Lin and G. W. Morgan, "Wave propagation through fluid contained in a cylindrical, elastic shell," *The Journal of the Acoustical Society of America*, vol. 28, no. 6, pp. 1165–1176, 1956.

[30] R. . ANSYS® Academic Research, "Help system, coupled field analysis guide," *ANSYS, Inc*, 2012.

[31] C. Lavooij and A. Tijsseling, "Fluid-structure interaction in compliant piping systems," in *Proceedings 6th BHRA International Conference on Pressure Surges (Cambridge, UK, October 4-6, 1989)*, A. Thorley, Ed. British Hydromechanics Research Association, 1990, pp. 85–100.

[32] A. Boresi, K. Chong, and J. D. Lee, *Elasticity in Engineering Mechanics*. Wiley, 2010.